



Lead-free $\text{Ba}_{0.9}\text{Ca}_{0.1}\text{Ti}_{0.9}\text{Zr}_{0.1}\text{O}_3$ piezoelectric ceramics processed below 1300 °C



A. Reyes-Montero ^{a,*}, L. Pardo ^b, R. López-Juárez ^{c,*}, A.M. González ^d, M.P. Cruz ^e, M.E. Villafuerte-Castrejón ^a

^a Instituto de Investigaciones en Materiales, Universidad Nacional Autónoma de México, Circuito Exterior S/N, A.P. 70-360 Coyoacán, México D.F., Mexico

^b Instituto de Ciencia de Materiales de Madrid, ICMM-CSIC, c/ Sor Juana Inés de la Cruz, 3, Cantoblanco, 28049 Madrid, Spain

^c Centro de Ciencias Aplicadas y Desarrollo Tecnológico, Universidad Nacional Autónoma de México, A.P. 70-186 Coyoacán, México D.F., Mexico

^d Grupo POEMA, EUIT Telecomunicación, Universidad Politécnica de Madrid, Ctra. Valencia Km. 7, 28031 Madrid, Spain

^e Centro de Nanociencias y Nanotecnología, Universidad Nacional Autónoma de México, Km. 107, Carretera Tijuana-Ensenada, C.P. 22800 Ensenada, B.C., Mexico

ARTICLE INFO

Article history:

Received 28 May 2013

Received in revised form 22 August 2013

Accepted 26 August 2013

Available online 13 September 2013

Keywords:

Ferroelectrics

Piezoelectricity

Ceramics

Pechini method

ABSTRACT

$\text{Ba}_{0.9}\text{Ca}_{0.1}\text{Ti}_{0.9}\text{Zr}_{0.1}\text{O}_3$ (BCTZ) lead-free piezoelectric ceramics were successfully prepared by Pechini polymeric precursor method using low thermal treatments. XRD analysis shows single-phase perovskite type structure for powders synthesized at 700 °C for 1 h. Dense ceramics were obtained from these reactive precursors using sintering temperatures below 1300 °C (1200 °C, 1250 °C and 1275 °C for 5 h). The ceramics sintered at 1275 °C for 5 h exhibited the best ferro–piezoelectric properties: $d_{33} = 390$ pC/N, $d_{31} = -143$ pC/N, $k_p = 50\%$, $\epsilon_{33}^T = 2253$ and $\tan \delta = 0.06$ (100 kHz) at room temperature, $T_C = 112$ °C, $2P_r = 24$ $\mu\text{C}/\text{cm}^2$ and $2E_C = 4.07$ kV/cm. Dense ceramics sintered at 1250 °C for 5 h (97% theoretical density) have average grain size ≈ 5 μm , $T_C = 115$ °C and high ferro–piezoelectric performance ($d_{33} = 340$ pC/N, $k_p = 49\%$). The high piezoelectric sensitivity is due to the high polarizability of the ceramics at local level.

© 2013 Elsevier B.V. All rights reserved.

1. Introduction

The development of lead-free ceramic materials with high piezoelectric sensitivity remains to date as a primary scientific challenge driven by the toxicity of lead oxide, and, nowadays, directives for environmental protection [1]. Barium titanate (BT), a classical lead-free ferroelectric (FE) [2], has been widely studied because of its important properties applied to several electronic components, but its piezoelectric properties cannot compete with those of commercial ceramics. A number of chemical substitutions of the A and/or B sites of the BT perovskite structure have been made to tailor the electrical properties by appropriated shifting the temperatures of the rhombohedral-to-orthorhombic (T_1), FE–FE, the orthorhombic-to-tetragonal (T_2), FE–FE, and the tetragonal-to-cubic (T_C), FE–paraelectric phase transitions [2].

Dopants, such as Ca^{2+} in A-site up to 24 at.%, reduces T_1 and T_2 , causing little modification of the Curie temperature (T_C), and thus, stabilizing the tetragonal FE phase at room temperature [3], while doping the B-site produce an undesired reduction of T_C [4]. Therefore substitution of B-site with Zr^{4+} (BZT) improves the piezoelectric parameters because the three phase transition temperatures

get together below room temperature at 15 at.% of Zr^{4+} content [5], which gives place to phases coexistence and causes instability in the polarization state. Such effect should promote an easily reorientation of the domains during the poling process and enhanced piezoelectricity, similar to the morphotropic phase boundary (MPB) of lead titanate–zirconate (PZT) or the polymorphic phase boundary (PPB) of sodium–potassium niobate (KNN).

Zr^{4+} substitution also promotes a dielectric relaxor behavior that limits this effect [5,6]. Relaxor behavior is linked with the existence of polar nanoregions (PNRs) which have distinct symmetry than the average structure. In fact, Extended X-ray Absorption Fine Structure (EXAFS) and Atomic Pair Distribution Function (PDF) analyses on BZT showed that structural distortion arises due to the $\text{Ti}^{4+}/\text{Zr}^{4+}$ size mismatch and the local structure is distinct from the average long-range structure [7,8].

Recently, by a combination of A and B sites substitution, high-performance lead-free ceramics in the pseudo-binary solid-solution system $(1-x)\text{Ba}(\text{Zr}_y\text{Ti}_{1-y})\text{O}_3-x(\text{Ba}_{1-z}\text{Ca}_z)\text{TiO}_3$ (BZT–xBCT) are being developed and extensively studied [9–14]. In particular, $(1-x)\text{Ba}(\text{Zr}_{0.2}\text{Ti}_{0.8})\text{O}_3-x(\text{Ba}_{0.7}\text{Ca}_{0.3})\text{TiO}_3$, which show a high piezoelectric coefficient d_{33} of ~ 620 pC/N at $x = 0.50$ (i.e. $\text{Ba}_{0.85}\text{Ca}_{0.15}\text{Ti}_{0.90}\text{Zr}_{0.10}\text{O}_3$) has been reported [9]. Such composition stays at the vicinity of a tricritical point of this system, in the frontier of the high temperature cubic non-ferroelectric phase, with the two ferroelectric ones, rhombohedral and tetragonal phases. It has been suggested that there is a coexistence of the cubic phase with the

* Corresponding authors. Tel.: +52 55 56 22 46 41x24646; fax: +52 55 56 16 13 71.

E-mail addresses: ingaremo@gmail.com (A. Reyes-Montero), rigobertolj@yahoo.com.mx (R. López-Juárez).

two ferroelectric ones enhancing the polarizability of the ceramic. In addition to the polarization rotation mechanism (rhombohedral–tetragonal) there would be an additional mechanism of polarization extension (cubic–tetragonal and cubic–rhombohedral) [15].

The drawbacks of this composition for being amenable for commercial processing and practical use are the low Curie temperature $T_C \sim 93^\circ\text{C}$ and the high synthesis (1300°C for 2 h) and sintering (1450°C for 3 h) temperatures. Some works have been focused on increasing T_C (up to 114°C) at the expenses of the piezoelectric performance (down to 450 pC/N) by changing the composition to $(1-x)\text{Ba}(\text{Zr}_{0.15}\text{Ti}_{0.85})\text{O}_3-x(\text{Ba}_{0.7}\text{Ca}_{0.3})\text{TiO}_3$ with $x = 0.53$ (i.e. $\text{Ba}_{0.84}\text{Ca}_{0.16}\text{Ti}_{0.93}\text{Zr}_{0.07}\text{O}_3$), and still sintering at 1450°C for 3 h [10]. Nevertheless, sintering these ceramics at lower temperatures is a difficult task. Nowadays, state of the art on low temperature processing using conventional ceramic technology is that $\text{Ba}_{0.85}\text{Ca}_{0.15}\text{Ti}_{0.90}\text{Zr}_{0.10}\text{O}_3$ ceramics, including CeO_2 addition, calcined at 1250°C for 2 h and sintered at 1350°C for 4 h possesses a piezoelectric coefficient $d_{33} \approx 600\text{ pC/N}$ [11] or $\text{Ba}_{0.85}\text{Ca}_{0.15}\text{Ti}_{0.90}\text{Zr}_{0.10}\text{O}_3$ ceramics, including MnO addition, calcined at 1100°C for 4 h and sintered at 1350°C for 2 h possesses a piezoelectric coefficient $d_{33} \approx 373\text{ pC/N}$ [12]. Also LiF , Ga_2O_3 and Y_2O_3 have been added to $\text{Ca}^{2+}\text{-Zr}^{4+}$ doped BaTiO_3 ceramics with sintering temperatures ranging from 1350 to 1500°C and d_{33} over $360\text{--}440\text{ pC/N}$ were obtained [16–18].

As an alternative to conventional solid state synthesis and in order to reduce the processing temperatures, the Pechini method has been recently used to obtain BCTZ ceramic materials [13]. This technique is based on having individual cations complexed with poly-functional organic acids (citric acid is preferred) and a poly-hydroxyl alcohol (commonly ethyleneglycol). The effectiveness of this method is maintaining ions mixed at atomic level when they form a polymer resin after heating around $80\text{--}110^\circ\text{C}$. This resin can be calcined at low temperature ($500\text{--}800^\circ\text{C}$) to produce very fine powders with narrow crystal size distribution.

In this work, $\text{Ba}_{0.9}\text{Ca}_{0.1}\text{Ti}_{0.9}\text{Zr}_{0.1}\text{O}_3$ ceramics have been synthesized by the Pechini route and sintered at temperatures below 1300°C , which facilitates the commercial use of these lead-free and high sensitivity ceramics. The effects of reducing synthesis and sintering temperatures on the structure, microstructure and electrical properties are discussed.

2. Experimental details

BCTZ powders were prepared by Pechini polymeric precursor method. $\text{Zr}(\text{OC}_3\text{H}_7)_4$ (70% in 1-propanol) and $\text{Ti}[\text{OCH}(\text{CH}_3)_2]_4$ were mixed using absolute (99.9%) ethyl alcohol as solvent. Also, $(\text{CH}_3\text{COO})_2\text{Ba}$ (99.0%) and $\text{Ca}(\text{NO}_3)_2 \cdot 4\text{H}_2\text{O}$ (99.8%) were mixed using deionized water and added to the first solution. Immediately, citric acid ($\text{C}_6\text{H}_8(\text{COOH})_3$ –99.5%) and ethylene-glycol ($\text{C}_2\text{H}_6\text{O}_2$ –99.0%) in a 3:1 M ratio were incorporated to the above solution. Then, this solution was stirred at room temperature for 30 min. The mixture was heated at 60°C until it gradually became transparent. After that, the temperature was raised to 70°C for evaporating solvents, until a yellow viscous resin was obtained. Then temperature was raised again to 85°C in order to promote the polymerization of the material. The resin was pre-calcined at 300°C for 30 min obtaining dark-brown powders. The powders were further calcined at 700°C for 1 h and ball milled for 8 h with zirconia ball media and alcohol. After that, they were dried and pressed into pellets of 13.0 mm diameter. Then, these samples were sintered at 1200°C , 1250°C and 1275°C for 5 h.

The crystal structure of the ceramics was examined using X-ray diffraction with a $\text{Cu } K\alpha_1$ radiation (1.54178 \AA , Bruker D8 Advance with a 0.016 step size and 1 s integration time). The morphology of the samples was observed by field emission Scanning Electron Microscope (JEOL-J7600f) and computer aided image analysis using *Image J* software. Average grain size of a large sample area was determined by the interception method. The samples were polished and silver electrodes were painted in both circular faces and annealed at 600°C for 30 min for the dielectric and piezoelectric measurements. Before measuring the piezoelectric properties, the sintered ceramics were poled under 2 kV/mm DC field at room temperature. The dielectric permittivity (ϵ'_{33}) and losses ($\tan\delta$) were measured with a precision impedance analyzer (Agilent 4294A) from room temperature up to 220°C . The piezoelectric constant d_{33} was measured after 24 h of the poling process using a d_{33} -meter (APC International). The d_{31} constant, as well as the electromechanical

coupling factor k_p , the elastic compliances s_{11}^E, s_{12}^E , the piezoelectric g_{31} constant and the frequency number N_p were calculated using the resonance method and an automatic iterative analysis method of the complex impedance at the radial mode [19]. Ferroelectric hysteresis loops were measured at room temperature using a Radiant RT66 workstation at 100 Hz .

3. Results and discussion

Fig. 1 shows the XRD patterns of BCTZ powders calcined at 700°C for 1 h and sintered at different temperatures for 5 h. All samples showed single-phase perovskite crystal structure at the technique resolution. The diffraction peaks of the samples were indexed belonging to the perovskite-type tetragonal structure with space group $P4mm$ in agreement with recent literature [20]. Fig. 2 is a magnification around the 002/200 doublet of the BT-like tetragonal structure. The wide and strongly asymmetric peak around 45° for the ceramic sintered at 1200°C indicates the 002/200 doublet of the tetragonal structure at room temperature. The subtle shift of diffraction peaks to lower angles as the sintering temperature increases in Fig. 2 indicates the expansion of the cell volume. This also indicates a more effective substitution of Ti^{4+} , with 0.605 \AA ionic radius, by Zr^{4+} , with 0.72 \AA ionic radius in octahedral coordination, for the higher sintering temperature, which will give place to a cell volume increase. It is plausible that the residual Zr^{4+} for the lower sintering temperature materials could be present at grain boundaries in small amount as secondary phase, undetectable by XRD.

The 002/200 tetragonal doublet seen for the ceramic sintered at 1200°C merge into a symmetric single peak for the sample sintered at 1275°C , which indicates a pseudo-cubic structure. Such a pseudo-cubic structure is not compatible with the ferro–piezoelectric performance.

Fig. 2 also shows the effect of the electric field in the structure, obtained after removing the electrode used for poling. For the ceramic sintered at 1200°C , the 002/200 peak has higher asymmetry, which shows that the 002 peak is more intense in the poled ceramic revealing the well-know effect of texture change by domain reorientation under the electric field. However, there is no effect of the poling on the structure of the ceramic sintered at 1275°C . This seems to indicate that the electric field does not change the global symmetry of the ceramics. The XRD results obtained in this work are comparable with those reported before for similar compositions [21–24]. The splitting and intensity ratio of the 200/002 diffractions are considered as the coexistence of tetragonal and rhombohedral phases in different proportions depending of the composition.

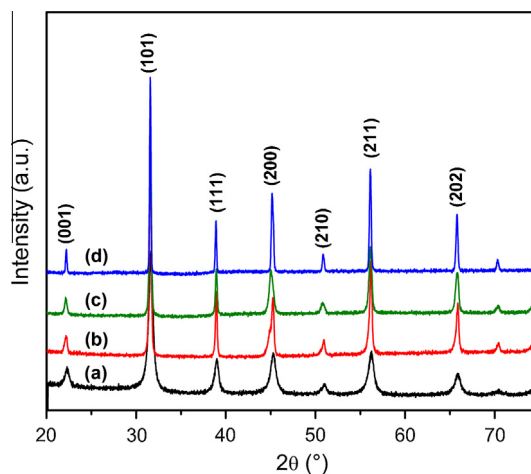


Fig. 1. XRD patterns of BCTZ ceramics: (a) calcined at 700°C for 1 h; and sintered for 5 h at: (b) 1200°C , (c) 1250°C and (d) 1275°C .

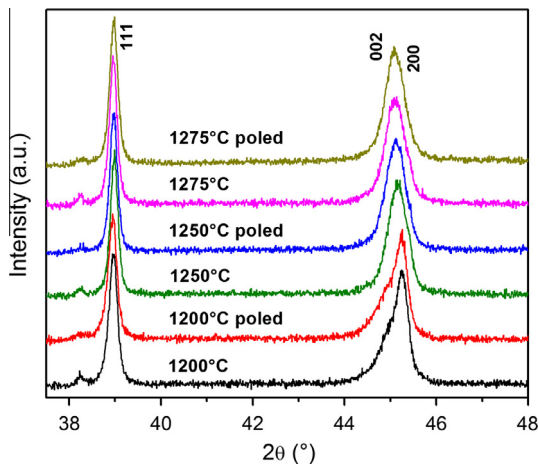


Fig. 2. Magnified XRD patterns of unpoled and poled ceramics in the 37.5–48° 2θ range.

Fig. 3 shows the SEM micrographs of BCTZ powders and ceramics sintered at different temperatures for 5 h. As expected, the ceramic microstructure changes with the sintering temperature. The average powder crystal size is around 50 nm, while the pellets sintered at 1200, 1250 and 1275 °C have 0.4, 4.6 and 15.2 μm , respectively. The theoretical density calculated with lattice parameters obtained from XRD patterns is 5.81 g/cm^3 . Measured relative densities in sintered samples were found between 95–98% as the sintering temperature increases.

Current work on BCTZ ceramics synthesized by conventional solid state reaction and using high sintering temperatures, commonly up to 1450 °C [9–10] or even higher [21], leads to large

grain microstructures (average crystal size $\sim 30 \mu\text{m}$). Recent work regarding relation between microstructure and properties in these ceramics, shown that below an average grain size $\sim 10 \mu\text{m}$, it is not possible to obtain BCZT ceramics with good piezoelectric properties [21]. However, coarse grained ceramics needs undesirable high sintering temperatures or complex two-steps sintering schedules to be produced and, besides, are not optimized for the present trend of miniaturization of devices based on piezoceramics, in order to increase the frequency range of the ultrasonic transduction.

The dielectric permittivity and losses as a function of temperature up to 220 °C are shown in Fig. 4. The data for the ceramic sintered at 1200 °C do not show an increase in permittivity near room temperature, expected in the proximity of a phase transition. This suggests that the combined Ca^{2+} incorporation in A-sites of the perovskite and some Zr^{4+} substitution made T_1 and T_2 phase transition temperatures of BT shift to lower values, below room temperature, whereas the Curie temperature undergoes a small change ($T_C = 118 \text{ °C}$) [3]. This is in agreement with the observed XRD patterns (Figs. 1 and 2) suggesting that the Ca^{2+} incorporation stabilizes the tetragonal phase at room temperature. The proper ferroelectric character of this structure is shown by the minor frequency dispersion shown in these permittivity curves. The fine grain size, in the sub-micron range, of the ceramic sintered at 1200 °C explains the reduction of the permittivity [21].

As the sintering temperature increases, the curves for the ceramics sintered at 1250 and 1275 °C show higher permittivity values, subtle reduction of T_C to 115 °C and 112 °C, respectively, and a higher frequency dispersion than the curves for the ceramic sintered at 1200 °C. Moreover, for higher sintering temperatures, and despite of the increase in grain size (Fig. 3), the maximum in permittivity at the phase transition is still broad. For the sample sintered at 1275 °C there is a soft anomaly in the permittivity curve at 42 °C, that could correspond to the phase transition from the

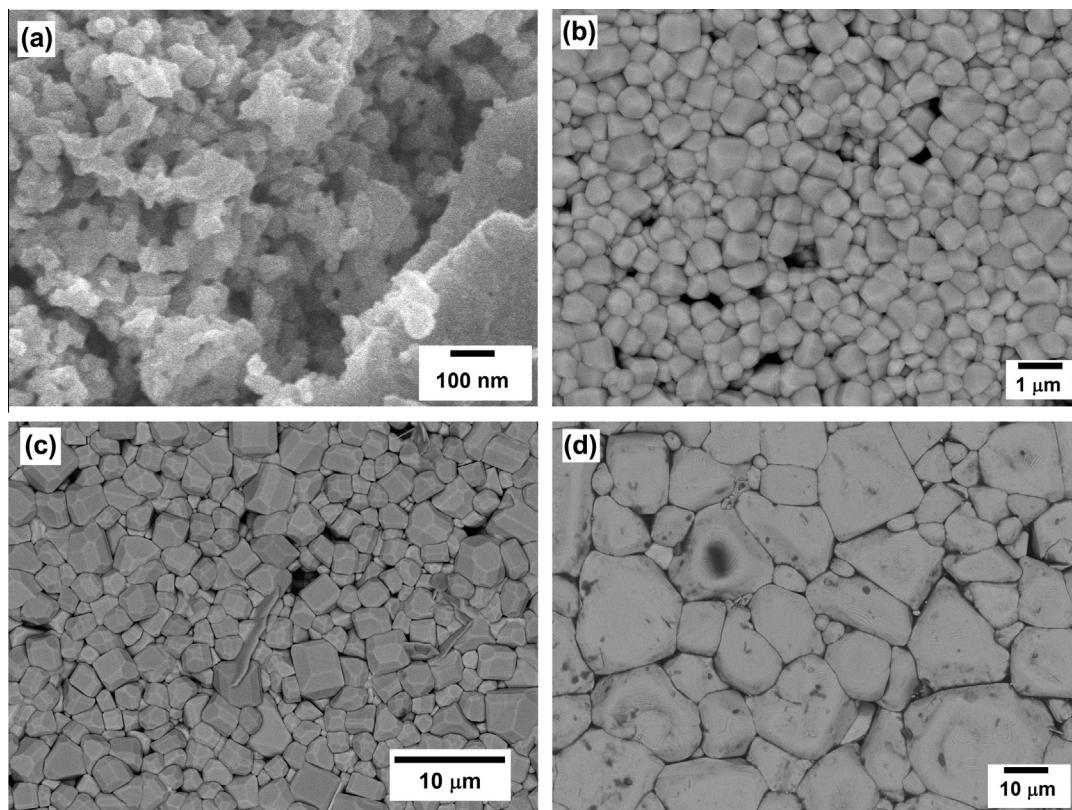


Fig. 3. SEM images for BCTZ ceramics: (a) calcined powders at 700 °C for 1 h; sintered ceramics for 5 h at: (b) 1200 °C, (c) 1250 °C and (d) 1275 °C.

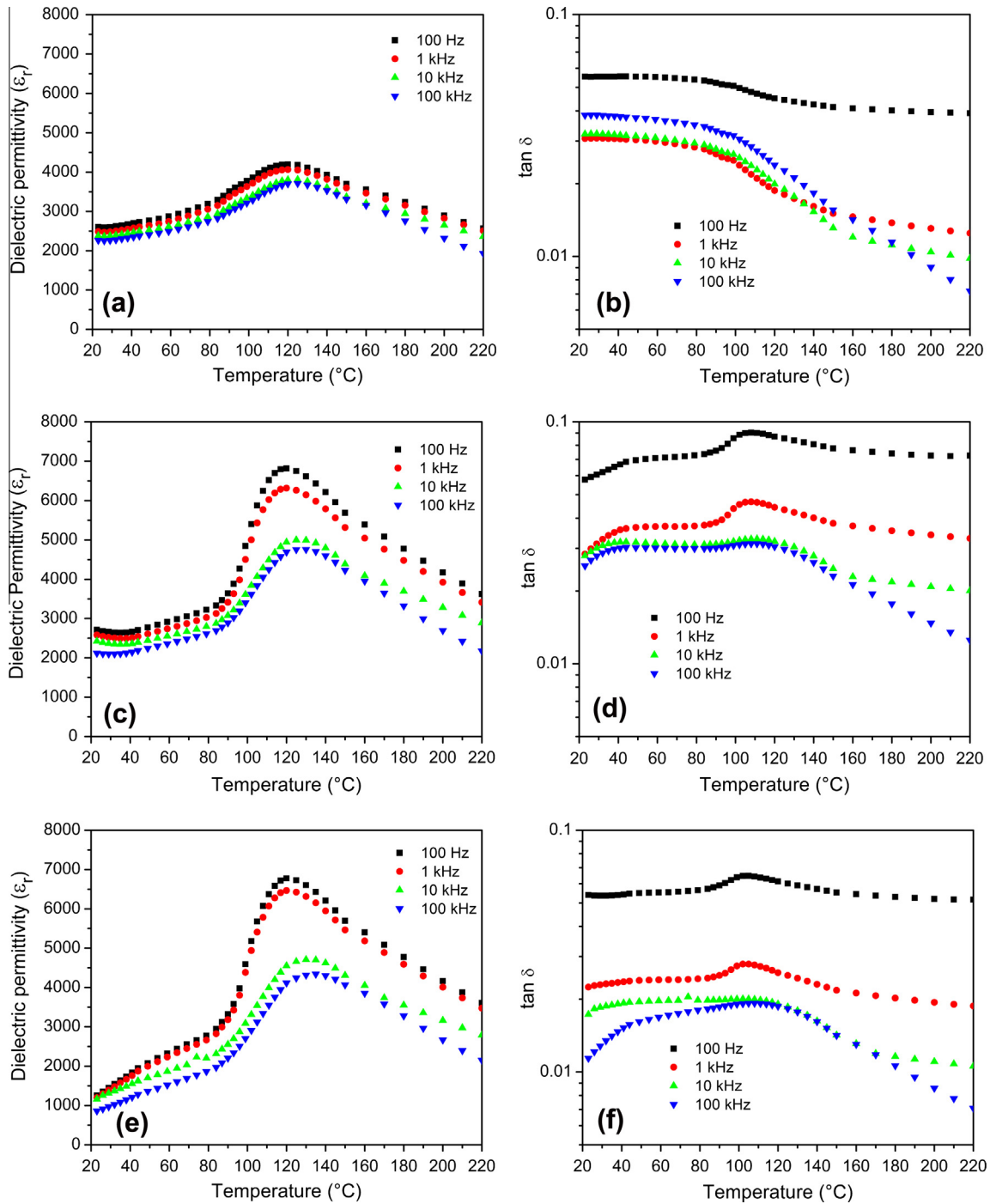


Fig. 4. Dielectric permittivity and losses of BCTZ sintered ceramics for 5 h at: (a–b) 1200 °C, (c–d) 1250 °C and 1275 °C (e–f).

rhombohedral to tetragonal ferroelectric phases (T_{R-T}). All these characteristics correspond to the diffuse transitions of systems which have a locally disordered structure, i.e., relaxor behavior. This is compatible with increasing amount of Zr^{4+} ions incorporation into the perovskite lattice [5,6] as the sintering temperature increases. The thermal evolution of the permittivity for the ceramics sintered at 1250 °C and 1275 °C show their ferroelectric character, with a transition from a polar to a non-polar phases at T_C , despite of the global pseudo-cubic crystal structure observed (Figs. 1 and 2).

Fig. 5 shows the P – E hysteresis loops of BCTZ ceramics recorded at room temperature. Loops for fine grained material sintered at

1200 °C show a small ferroelectric contribution with a remnant polarization $2P_r < 10 \mu\text{C}/\text{cm}^2$. However, as the sintering temperature increases the loops become well saturated and $2Pr$ increases to $\sim 24 \mu\text{C}/\text{cm}^2$ for ceramics sintered at 1250 and 1275 °C together with low coercive fields that indicates an easy polarization mechanism of the material.

The piezoelectric properties of BCTZ ceramics are summarized in Table 1. The values of piezoelectric constant d_{33} and the electro-mechanical coupling factor k_p are similar to those reported for similar compositions [21–23]. Fig. 6 shows the radial resonance spectra (real part of the impedance and phase angle as a function of the frequency) for the samples sintered at 1200 and 1250 °C

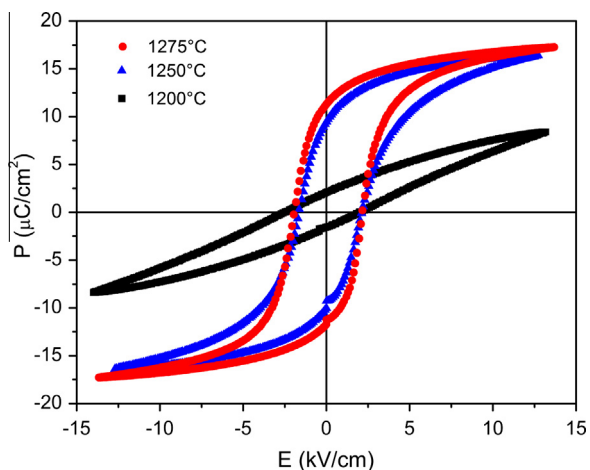


Fig. 5. Ferroelectric hysteresis loops of BCTZ sintered samples at different temperatures.

for 5 h. In agreement with the low polarization level of this ceramic (Fig. 5), the impedance spectra shows a very weak resonance, as a consequence of the very fine grain size (Fig. 3), in comparison with the observed for the ceramics sintered at higher temperatures. The smaller crystal size, and the corresponding smaller domain size, requires more energy for domain wall motion, as evidenced by the low dielectric permittivity, ferroelectric loop and the resonance spectra for this sample. Although the best properties are obtained for the ceramic sintered at 1275 °C, the ceramic sintered at 1250 °C already have the characteristics of a high sensitivity piezoelectric material. Both poled ceramics share the same crystal structure characteristics and the pseudo-cubic structure (Fig. 2) that is not compatible with a ferro–piezoelectric behavior. Current explanations of this apparent contradiction are in the coexistence of three phases if the studied composition were in the vicinity of a tricritical point. However the sharp (111) peak observed for these samples (see Fig. 2) could be pointing to the fact that a long-range rhombohedral phase is not present in the studied ceramics.

The explanation of the apparent contradiction of a pseudo-cubic structure together with a high ferro–piezoelectric response could be found by similitude with another high piezoelectric sensitivity complex compound, $0.5\text{Ba}(\text{Zr}_{0.2}\text{Ti}_{0.8})\text{O}_3-0.5(\text{Ba}_{0.7}\text{Ca}_{0.3})\text{TiO}_3$, i.e. $\text{Ba}_{0.85}\text{Ca}_{0.15}\text{Ti}_{0.90}\text{Zr}_{0.10}\text{O}_3$, for which detailed structural results were recently reported [21]. For this, the long-range structure observed by XRD does not fully represent the actual crystal structure due to local structural disorder caused by the large size mismatch between Zr^{4+} and Ti^{4+} ionic radii, as well as the inequality of the octahedral tilting between TiO_6 and ZrO_6 . This was first found in lead zirconate–titanate (PZT) [7] and BZT [8].

The global pseudo-cubic structure observed in the ceramics sintered at 1250 °C and 1275 °C could in fact average a range of local polar configurations. Both global and short-range structure is needed to understand the structural response under the electric field near a tricritical point, however, this is out the scope of this work. With similar structural features to other materials reported in the literature [25], we may speculate that for the high sensitivity

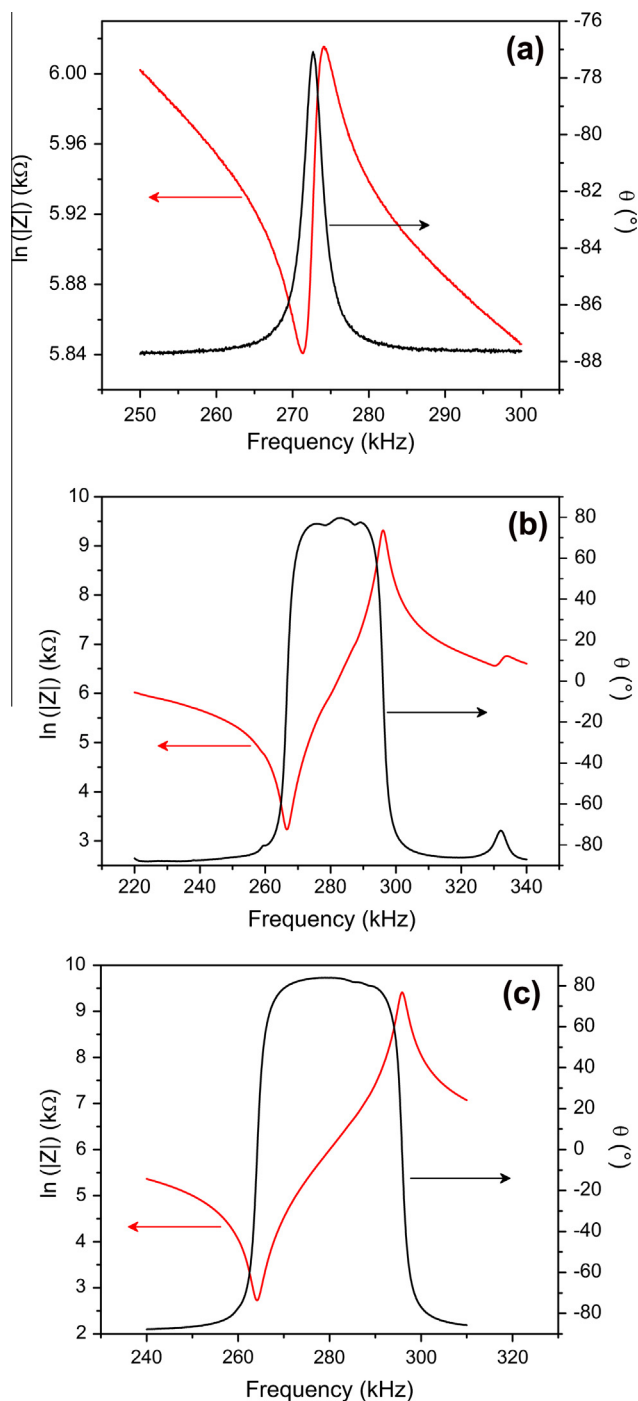


Fig. 6. Radial resonance spectra of sintered samples at: a) 1200, b) 1250 and c) 1275 °C for 5 h.

studied ceramics, the order–disorder type polarization mechanism couples with the strain, resulting in the large ferro–piezoelectric response.

Table 1
Properties of BCTZ sintered ceramics for 5 h.

Sintering temp. (°C)	ρ (g/cm ³)	d_{33} (10 ⁻¹² C/N)	d_{31} (10 ⁻¹² C/N)	k_p (%)	N_p (%)	s_{11}^E (10 ⁻¹² m ² /N)	s_{11}^E (10 ⁻¹² m ² /N)	g_{31} (10 ⁻³ V m/N)
1200	5.49	45	-14	5	2801	17.1	-9.8	-0.7
1250	5.64	240	-120	49	2691	11.4	-3.4	-6.4
1275	5.70	390	-143	50	2689	11.1	-2.9	-7.2

4. Conclusions

Summarizing, single-phase perovskite-type structure $\text{Ba}_{1-x}\text{Ca}_x\text{Zr}_{0.9}\text{Ti}_{0.1}\text{O}_3$ ceramic powder was synthesized by Pechini polymeric precursor method at 700 °C for 1 h. Dense ceramics (95%–98% theoretical density) were then obtained using low sintering conditions (1200 °C, 1250 °C, 1275 °C for 5 h). The tetragonal crystal structure at room temperature and the observed T_C at 118 °C of ceramics sintered at 1200 °C indicates that Ca^{2+} incorporation takes place in A-sites of the perovskite structure. The fine grain size of this ceramics explains the depletion of the permittivity curves and the reduced ferro–piezoelectric properties. For a complete Zr^{4+} incorporation and corresponding high sensitivity characteristics, higher sintering temperatures are needed. The XRD patterns and dielectric permittivity curves shows that ceramics obtained at 1250 °C and 1275 °C possesses a pseudo-cubic crystal structure and undergoes a ferroelectric-relaxor to a paraelectric phase transition at $T_C = 115$ °C and 112 °C, respectively, which indicates an increasing Zr^{4+} incorporation in the lattice. The low coercive field of ceramics sintered at 1250 and 1275 °C, together with their high piezoelectric properties, indicates that they are highly polarizable. The best piezoelectric properties are obtained for the ceramic sintered at 1275 °C ($d_{33} = 390$ pC/N, $d_{31} = -143$ pC/N, $k_p = 50\%$). The long-range pseudocubic structure observed by XRD may not fully represent the actual crystal structure due to local structural disorder caused by the large size mismatch between Zr^{4+} and Ti^{4+} ionic radii, as well as the inequality of the octahedral tilting between TiO_6 and ZrO_6 . This will give place to high local polarizability and piezoelectric sensitivity in these ceramics.

Acknowledgements

A. Reyes wants to thank to CONACyT-México for providing a MS. scholarship. M.E. Villafuerte-Castrejón kindly acknowledges

to PAPIIT-UNAM under project IN116610-3 and CONACyT CB-2011-1 No.166108 for financial support. L. Pardo acknowledges support of CSIC-PIE 201060E069.

References

- [1] J. Rödel, W. Jo, K.T.P. Seifert, E.M. Anton, T. Granzow, D. Damjanovic, *J. Am. Ceram. Soc.* 92 (2009) 1153–1177.
- [2] S. Roberts, *Phys. Rev.* 71 (1947) 890–895.
- [3] T. Mitsui, W.B. Westphal, *Phys. Rev.* 124 (1961) 1354–1359.
- [4] J.G. Park, T.S. Oh, Y.H. Kim, *J. Mater. Sci.* 27 (1992) 5713–5719.
- [5] Z. Yu, C. Ang, R. Guo, A.S. Bhalla, *J. Appl. Phys.* 92 (2002) 1489.
- [6] T. Maiti, R. Guo, A.S. Bhalla, *J. Am. Ceram. Soc.* 91 (2008) 1769–1780.
- [7] I. Grinberg, V.L. Cooper, A.M. Rappe, *Nature* 419 (2002) 909–911.
- [8] I.K. Jeong, C.Y. Park, J.S. Ahn, S. Park, D.J. Kim, *Phys. Rev. B* 81 (2010) 214119.
- [9] W. Liu, X. Ren, *Phys. Rev. Lett.* 103 (2009) 257602.
- [10] H. Bao, C. Zhou, D. Xue, J. Gao, X. Ren, *J. Phys. D: Appl. Phys.* 43 (2010) 465401.
- [11] Y. Cui, X. Liu, M. Jiang, X. Zhao, X. Shan, W. Li, C. Yuan, C. Zhou, *Ceram. Int.* 38 (2012) 4761–4764.
- [12] M. Jiang, Q. Lin, D.M. Lin, Q.J. Zheng, X.M. Fan, X.C. Wu, H.L. Sun, Y. Wan, L. Wu, *J. Mater. Sci.* 48 (2013) 1035–1041.
- [13] T.H. Hsieh, S.C. Yen, D.T. Ray, *Ceram. Int.* 38 (2012) 755–759.
- [14] Y. Tian, X. Chao, L. Wei, P. Liang, Z. Yang, *J. Appl. Phys.* 113 (2013) 184107.
- [15] D. Damjanovic, N. Klein, J. Li, V. Porokhonsky, *Funct. Mater. Lett.* 3 (2010) 5–13.
- [16] C.K. Ivan-Tan, K. Yao, J. Ma, *Int. J. Appl. Ceram. Technol.* 10 (2013) 701–706.
- [17] J. Ma, X. Liu, W. Li, *J. Alloys Comp.* 581 (2013) 642–645.
- [18] W. Li, J. Hao, W. Bai, Z. Xu, R. Chu, J. Zhai, *J. Alloys Comp.* 531 (2012) 46–49.
- [19] C. Alemany, A.M. Gonzalez, L. Pardo, B. Jimenez, F. Carmona, J. Mendiola, *J. Phys. D: Appl. Phys.* 28 (1995) 945–956.
- [20] A.B. Haugen, K.J. Bowman, J.S. Forrester, D. Damjanovic, B. Li, J.L. Jones, *J. Appl. Phys.* 113 (2013) 014103.
- [21] J. Hao, W. Bai, W. Li, J. Zhai, *J. Am. Ceram. Soc.* 95 (2012) 1998–2006.
- [22] W. Li, Z. Xu, R. Chu, P. Fu, G. Zang, *Mater. Sci. Eng. B* 176 (2011) 65–67.
- [23] J. Wu, D. Xiao, B. Wu, W. Wu, J. Zhu, Z. Yang, J. Wang, *Mater. Res. Bull.* 47 (2012) 1281–1284.
- [24] W. Li, Z. Xu, R. Chu, P. Fu, G. Zang, *J. Am. Ceram. Soc.* 93 (2010) 2942–2944.
- [25] I.K. Jeong, J.S. Ahn, *Appl. Phys. Lett.* 101 (2012) 242901.